STUDY ON MHD FLOW OF MICROPOLAR FLUID OVER A STRETCHING SURFACE UNDER THE IMPACTS OF HEAT SOURCE AND CHEMICAL REACTION

P. Roja[1], S. Venkateswarlu[2], Mani Ramanuja[3], T. Sankar Reddy[4], M. Parvathi[5], M. Umamaheswar[6], P. Chandra Reddy[7] A .B. Madhumohana Raju[8*]

Article History: Received: 01.04.2023 **Revised:** 05.05.2023 **Accepted:** 24.06.2023

Abstract

In this paper, the effects of thermal conductivity and chemical reaction on the magneto hydrodynamic flow of a micropolar fluid over a continuously moving stretching surface with heat source/sink are considered. The analysis accounts for thermophoresis and thermal radiation. The surface temperature is assumed to vary as a power-law temperature. The governing conservation equations of mass, momentum, angular momentum, energy and concentration are converted into a system of non-linear ordinary differential equations by means of similarity transformation. The resulting system of coupled non-linear ordinary differential equations is solved numerically. The numerical results show that the thermal boundary thickness increases as the thermal conductivity parameter S increases, while it decreases as the radiation parameter R increases. Also, it was found that the Nusselt and Sherwood numbers increase as R increases and decreases as S increases.

[1,5,6,7]Deparment of Mathematics, Annamacharya Institute of Technology and sciences, Rajampet, Kadapa-516126, Andhra Pradesh, India.
[2]Deparment of Mathematics and Statistics, Vignan's Foundation for Science, Technology and Research, Vadlamudi, Guntur-522213, Andhra Pradesh, India.
[3]Deparment of Mathematics, Marri Laxman Reddy Institute of Technology and Management, Dundigal, Hyderabad-5000043, India.
[4]Deparment of Mathematics, Annamacharya Institute of Technology and sciences, C. K. Dinne, Kadapa-516003, Andhra Pradesh, India.
[8*]Department of Mathematics, New Horizon College of Engineering, Bangalore - 560103, Karnataka, India.

*Corresponding Author Email: raju.madhuab@gmail.com

DOI: 10.31838/ecb/2023.12.6.85

1. INTRODUCTION

In many industrial manufacturing processes, the problem of heat and mass transfer in two-dimensional boundary layers on a continuous stretching surface, moving in an otherwise quiescent fluid medium, have attracted considerable attention during the last few decades. Examples may be found in continuous casting, glass-fiber production, metal extrusion, hot rolling, wire drawing, paper production, drawing of plastic films, metal and polymer extrusion and metal spinning [1–3]. Sakiadis [4] first investigated boundary layer flow over a continuous solid surface moving with constant speed. This problem was extended by Erickson et al. [5] and Fox et al. [6] to include the wall suction or injection and explained its effects on the heat and mass transfer in the boundary layer. Crane [7] first studied the flow caused by an elastic sheet whose velocity varies linearly with the distance from a fixed point on the sheet. Gupta and Gupta [8] presented the heat and mass transfer corresponding to the similarity solution for the boundary layer over a stretching sheet subject to suction or blowing. Chen and Char [9] investigated the effects of the variable surface temperature and variable surface heat flux on the heat transfer characteristics of a linearly stretching sheet subject to blowing or suction. Chakrabarti and Gupta [10] analysed the hydromagnetic flow and heat transfer over a stretching sheet. All of the above investigators restricted their analysis to flows of a Newtonian fluid.

In last two decades, a new stage in the evaluation of fluid dynamic theory is in excellent progress because of the increasing importance in the processing industries and elsewhere of materials whose flow shear behavior cannot be characterized by Newton relationships. The theory of micropolar fluids was first introduced and formulated by Eringen [11]. This theory display the effects of local rotary inertia and couple stress. The theory is expected to provide a mathematical model for the non-Newtonian fluid behavior observed in certain fluid such as exotic lubricants, polymeric fluid, colloidal fluids, liquid crystals, ferroliquid, etc., which is more realistic and important from a technological point of view. The theory of thermomicropolar fluids was developed by Eringen [12] by extending his theory of micropolar fluid. The flow characteristics of the boundary layer of micropolar fluid over a semi-infinite plate in different situations have been studied by many authors in Refs. [13–21].

At high operating temperatures, radiation effects can be quite significant. We know that the radiation effect is important under many non-isothermal situations. If the entire system involving the polymer extrusion process is placed in thermally controlled environment, then radiation could become important. The knowledge of radiation heat transfer in the system can perhaps lead to a desired product with a sought characteristic. Radiation effects on Newtonian and non-Newtonian fluids with and without magnetic field has been considered by many authors [22–27].

Thermophoresis is a mechanism of particle deposition, besides other ones like inertial impaction, sedimentation, Brownian diffusion etc. Thermophoresis phenomenon has many engineering applications in removing small particles from gas streams, in determining exhaust gas particle trajectories from combustion devices, and in studying the particulate material deposition on turbine blades. Duwairi and Damesh [28] investigated the effects of thermophoresis particle deposition on mixed convection from vertical surfaces embedded in saturated porous medium. Rahman et al. [29] analyzed the local similarity solutions for unsteady two-dimensional forced convective heat and mass transfer flow along a wedge with thermophoresis. Very recently, Adrian Postelnicu [30] studied the thermophersis partical deposition in natural convection over inclined surfaces in porous media.

The combined heat and mass transfer problems with chemical reaction are of importance in many processes and have, therefore, received a considerable amount of attention in recent years. In processes, such as drying, evaporation at the surface of a water body, energy transfer in a wet cooling the tower, and the flow in a desert cooler, the heat and mass transfer occurs simultaneously. Das *et al.* [31] considered the effects of first order chemical reaction on the flow past an impulsively started infinite vertical plate with constant heat flux and mass transfer.

Muthucumarswamy and Ganesan [32] and Muthucumarswamy [33] studied first order homogeneous chemical reaction on flow past infinite vertical plate. Ibrahim et al. [34] presented the effects of the chemical reaction and radiation absorption on the unsteady MHD free convection flow past a semi-infinite vertical permeable moving plate with heat source and suction. Demesh et al. [35] investigated combined effect of heat generation or absorption and first-order chemical reaction on micropolar fluid flow over a uniformly stretched permeable surface. Pal et al. [36] used perturbation analysis to study unsteady magnetohydrodynamic convective heat and mass transfer in a boundary layer slip flow past a vertical permeable plate with thermal radiation and chemical reaction. The buoyancy and chemical reaction effects on MHD mixed convection heat and mass transfer in a porous medium with thermal radiation and Ohmic heating was investigated by Pal and Talukdar [37].

In all of the previous studies the effects of thermal radiation and chemical reaction on MHD mixed convective flow of a micropolar fluid over a stretching surface with variable thermal conductivity were not studied. Hence, the aim of this work is to study the influence of temperature dependent thermal conductivity, chemical reaction and thermal radiation on MHD flow and mass transfer of a micropolar fluid over a continuously moving stretching surface in the presence of heat generation or absorption with suction or injection.

2. BASIC EQUATIONS

Consider a steady two-dimensional flow of an incompressible, electrically conducting micropolar fluid, subject to a transverse magnetic field over a semi-infinite stretching plate with variable temperature in the presence of radiation. The x-axis is directed along the continuous stretching plate and points in the direction of motion. The y-axis is perpendicular to x-axis and to the direction of the slot (the z-axis) whence the continuous stretching plate issues. It is assumed that the induced magnetic field and the Joule heating are neglected. The fluid properties are assumed to be constant, except for the fluid thermal conductivity which is taken as a linear function of temperature. Then under the usual boundary layer approximations, the governing equations for the problem can be written as follows [35]:

(i) Continuity

$$\frac{\partial u}{\partial x}+\frac{\partial v}{\partial y}=0 \tag{1}$$

(ii) Linear momentum

$$u\frac{\partial u}{\partial x}+v\frac{\partial u}{\partial y}=\left(\upsilon+\frac{K_1}{\rho}\right)\frac{\partial^2 u}{\partial y^2}+g\beta_T(T-T_\infty)+g\beta_C(C-C_\infty)+K_1\frac{\partial N}{\partial y}-\frac{\sigma B_0^2}{\rho}u \tag{2}$$

(iii) Angular momentum

$$G_1\frac{\partial^2 N}{\partial y^2}-2N-\frac{\partial u}{\partial y}=0 \tag{3}$$

(iv) Energy:

$$u\frac{\partial T}{\partial x}+v\frac{\partial T}{\partial y}=\frac{k}{\rho c_p}\frac{\partial^2 T}{\partial y^2}-\frac{1}{\rho c_p}\frac{\partial q_r}{\partial x}+\frac{Q_0}{\rho c_p}\left(T-T_\infty\right) \tag{4}$$

(iv) Concentration:

$$u\frac{\partial C}{\partial x}+v\frac{\partial C}{\partial y}=D\frac{\partial^2 C}{\partial y^2}-\frac{\partial(V_T C)}{\partial y}-Kr^*\left(C_w-C_\infty\right) \tag{5}$$

where u and v are the velocity components in the x and y directions respectively, $\nu=\left(\mu+S\right)/\rho$ is the apparent kinematic viscosity, μ is the fluid density, S a constant characteristic of the fluid, g is the acceleration due to gravity, ρ is the density of the fluid, σ is the electrical conductivity, B_0 is the externally imposed magnetic field in the y-direction, β_f and β_c are the thermal and concentration expansion coefficients, T , T_w and T_∞ is the temperature of the fluid inside the thermal boundary layer, the plate temperature and the fluid temperature in the free stream, respectively. G_1(>0) is the microrotation constant, N is the components of microrotation or angular velocity whose rotation is in the direction of the xy–plane, $K_1 = S/\rho(K_1 > 0)$ is the coupling constant, S is a constant characteristic of the fluid, Q_0 is the heat generation (>0) or absorption (<0) coefficient, While C , C_w and C_∞ are the corresponding spices concentration, k is the thermal conductivity, c_p is the specific heat at constant pressure, q_r is the radiative heat flux in the y –direction, D is the molecular diffusivity, V_T is the thermophoretic velocity, Kr^* is the rate of chemical reaction, $Kr^* > 0$ represents for destructive reaction, $Kr^* < 0$ represents for generative reaction and $Kr^* = 0$ represents for no reaction.. The second and third terms on the RHS of concentration equation (5) represent the thermophoresis and chemical reaction effects, respectively.

The appropriate boundary conditions for the above model are as follows:

$$\begin{aligned} &u = U_w = ax,\ v = v_0,\ \sigma = 0,\ T = T_w, C = C_w \ \ at\ y = 0, \\ &u = 0,\ v = 0,\ \sigma = 0,\ \ T = T_\infty\ ,\ C = C_\infty \ \ \ as\ y \to \infty \end{aligned} \tag{6}$$

where $U_w = ax$ is the velocity of the stretching sheet and v_0 is the suction/injection velocity. The wall temperature is assumed to vary along the plate according to the following power-law

$$T_w - T_\infty = \beta x^\gamma \tag{7}$$

where β and γ (the surface temperature parameter) are constants. The fluid thermal conductivity is assumed to vary as a linear function of the temperature in the form [44]

$$k = k_\infty[1 + b(T - T_\infty)] \tag{8}$$

where b is a constant depending on the nature of the fluid and k_∞ is the ambient thermal conductivity. In general, $b > 0$ for air and liquids such as water, while $b < 0$ for fluids such as lubrication oils.

By using the Rosseland approximation [45], we have

$$q_r = -\frac{4\sigma_s}{3k_e}\frac{\partial T^4}{\partial Y} \tag{9}$$

where σ_s the Stefan-Boltzmann constant and k_e the mean absorption coefficient.
It should be noted that by using the Rosseland approximation, the present analysis is limited to optically thick fluids. If the temperature differences within the flow are sufficiently small, then Equation (6) can be linearized by expanding T^4 into the Taylor series about T_∞, which after neglecting higher order terms takes the form

$$T^4 \cong 4T_\infty{}^3 T - 3T_\infty{}^4 \tag{10}$$

In view of Equations (9) and (10), Eq. (4) reduces to

$$u\frac{\partial T}{\partial x}+v\frac{\partial T}{\partial y}=\alpha\frac{\partial^2 T}{\partial y^2}+\frac{16\sigma T_\infty^3}{3\rho c_p k_1}\frac{\partial^2 T}{\partial y^2}+\frac{Q_0}{\rho c_p}\left(T-T_\infty\right) \tag{11}$$

Now the thermophoretic velocity V_T , which appears in the Eq. (4) can be written as [43]:

$$V_T=-kv\frac{\nabla T}{T_{ref}}=\frac{-kv}{T_{ref}}\frac{\partial T}{\partial y} \tag{12}$$

where T_{ref} is a reference temperature and k is the thermophoretic coefficient with range of value from 0.2 to 1.2 as indicated by Batchelor and Chen [42] and is defined from the theory of Talbot et al. [41] by

$$k=\frac{2Cs\left(\lambda_g/\lambda_p+C_tK_n\right)\left[1+K_n\left(C_1+C_2e^{-C_3/K_n}\right)\right]}{\left(1+3C_mK_n\right)\left(1+2\lambda_g/\lambda_p+2C_tK_n\right)} \tag{13}$$

where C_1, C_2, C_3, C_m, C_s, C_t are constants, λ_g and λ_p are the thermal conductivities of the fluid and diffused particles respectively and K_n is the Knudsen number.
A thermophoretic parameter τ can be defined as follows [43]:

$$\tau=\frac{-k\left(T_w-T_\infty\right)}{T_r} \tag{14}$$

Typical values of τ are 0.01, 0.05 and 0.1 corresponding to approximate values of $-k\left(T_w-T_\infty\right)$ equal to 3K, 15K and 30 K for a reference temperature of $T_r=300K$.
In order to write the governing equations and the boundary conditions in dimensionless form, the following non-dimensional quantities are introduced.

$$u=ax\,f'(\eta),v=-\sqrt{av}xf(\eta),\eta=\sqrt{\frac{a}{v}}y,\psi=(av)^{1/2}xf(\eta)$$
$$\theta(\eta)=\frac{T-T_\infty}{T_w-T_\infty},\ \phi(\eta)=\frac{C-C_\infty}{C_w-C_\infty},N=\left(\frac{\alpha^3}{v}\right)^{1/2}x\omega(n) \tag{15}$$

The continuity equation (1) is automatically satisfied by the Cauchy-Riemann Equations $u=\frac{\partial\psi}{\partial y}$ and $v=-\frac{\partial\psi}{\partial x}$.
In view of the Equation (15), and following the analysis of El-Arabawy, [11], the equations (2), (3), (5) and (11) reduce to the following non-dimensional form

$$\left(1+K\right)f'''+ff''+Gr\theta+Gc\phi+Kg'-Mf'=0 \tag{16}$$
$$G\omega''-(2\omega+f'')=0 \tag{17}$$
$$\left[4+3R\left(1+S\theta\right)\right]\theta''+3R\,\mathrm{Pr}\left(f\theta'+\delta\theta\right)=0 \tag{18}$$
$$\phi''+Sc\left\{f\phi'-\tau\theta'\right\}\phi'-Sc\left\{\tau\theta''-Kr\right\}\phi=0 \tag{19}$$

For air $0\le S\le 6$, for water $0\le S\le 0.12$, and for lubrication oils $-0.1\le:S\le 0$ [30].

The corresponding dimensionless boundary conditions are

$$\begin{aligned} &f(0)=f_w,\ f'(0)=1, g(0)=0,\ \theta(0)=1, \phi(0)=1, \\ &f'(\infty)=0,\ g(\infty)=0,\ \theta(\infty)=0,\ \phi(\infty)=0 \end{aligned} \tag{20}$$

In the previous equations, prime indicates differentiation with respect to η,

Where $f_w=\dfrac{v_0}{\sqrt{a\upsilon}}$ is the permeability of the porous surface which is positive for suction and negative for injection.

$M=\dfrac{\sigma B_0^2}{\rho a}$ is the magnetic Parameter,

$G_1=\dfrac{K_1}{\rho}$ is the coupling constant parameter,

$G=\dfrac{G_1 a}{\upsilon}$ is the microrotation parameter,

$\Pr=\dfrac{\mu c_p}{k}$ is the Prandtl number,

$R=\dfrac{kk_*}{4\sigma_* T_\infty^3}$ is the radiation parameter,

$S=b\left(T_w-T_\infty\right)$ is the thermal conductivity parameter,

$\delta=\dfrac{Q_0}{(\rho c_p)a}$ is the heat generation ($\delta>0$) or absorption ($\delta<0$) parameter.

$Sc=\dfrac{\nu}{D}$ is the Schmidt number,

and $Kr=\dfrac{Kr^*\upsilon}{Da}$ is the chemical reaction parameter.

To analyze the behavior of fluid at surface results are constructed for the physical quantity of interest. The skin-friction coefficient, couple stress, Nusselt number (rate of heat transfer) and Sherwood number (rate of mass transfer) are important physical parameters for this type of boundary layer flow.

From the velocity field, the skin-friction at the plate can be obtained, which in non-dimensional form is given by

$$C_f=\frac{\left(\mu+K\right)\left(\dfrac{\partial u}{\partial y}\right)_{y=0}+K\left(N\right)_{y=0}}{\left(1/2\right)\rho U_o^2}=-2\operatorname{Re}_x^{-(1/2)}\left(1+\frac{1}{\beta}\right)f''(0) \tag{21}$$

From the angular velocity field in the boundary layer, we can now calculate the couple stress coefficient at the wall of the plate, which in the non-dimensional form is given by

$$C_w=\frac{(\gamma/K)\left(\partial N/\partial y\right)_{y=0}}{\gamma U_0^3(2K\nu^2)}=\operatorname{Re}_x^{-1}\omega'(0) \tag{22}$$

From the temperature field, the rate of heat transfer coefficient can be obtained, this in non-dimensional form, in terms of the Nusselt number, is given by

$$Nu_x=\frac{-k\left(\dfrac{\partial T}{\partial y}\right)_{y=0}-\dfrac{4\sigma}{3k}\left(\dfrac{\partial T^4}{\partial y}\right)_{y=0}}{k\left(T_w-T_\infty\right)}=-\operatorname{Re}_x^{1/2}\left(1+\frac{4}{3R}\right)\theta'(0) \tag{23}$$

From the concentration field, the rate of mass transfer coefficient can be obtained, which in non-dimensional form, in terms of the Sherwood number, is given by

$$Sh_x = \frac{-D\left(\frac{\partial C}{\partial y}\right)_{y=0}}{U_0 C_\infty} = -\left(\mathrm{Re}_x^{-(1/2)}\right)\phi'(0) \qquad (24)$$

where $\mathrm{Re}_x = \frac{U_0 x}{\nu}$ is the Reynolds number

3. NUMERICAL TECHENIQUE

The set of coupled non-linear governing boundary layer equations (16) - (19) together with the boundary conditions (20) are solved numerically by using Runge-Kutta fourth order technique along with shooting method. The computations were done by a program which uses a symbolic and computational computer language (Mathematica 11.0) on a Pentium 1 PC machine. The step size $\Delta\eta = 0.01$ is used to obtain the numerical solution with five decimal place accuracy as the criterion of convergence. From the process of numerical computation, the skin-friction coefficient, the plate couple stress, the Nusselt number and the Sherwood number, which are respectively proportional to $f''(0), g'(0), -\theta'(0)$ and $-\phi'(0)$ are also sorted out and their numerical values are presented in a tabular form.

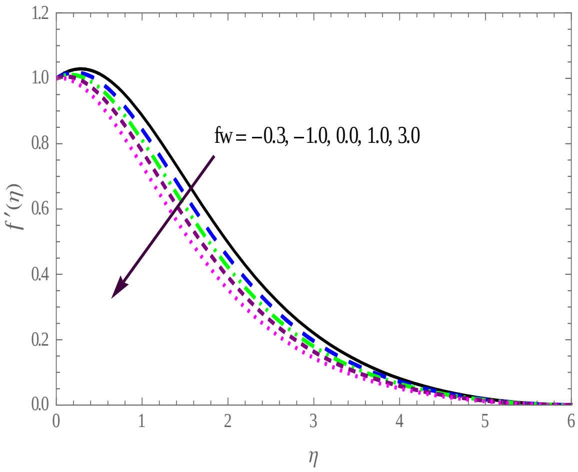

Fig.1(a). Effect of fw on velocity

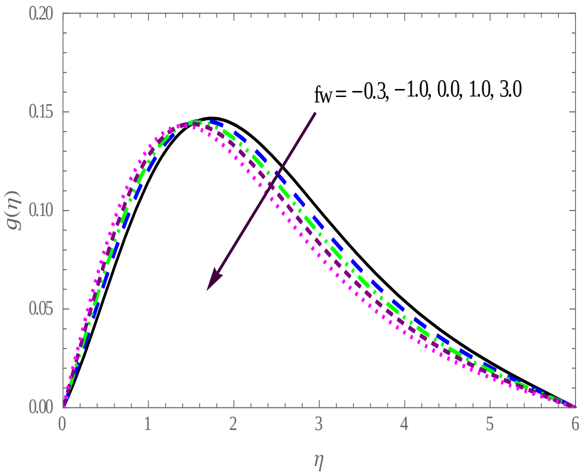

Fig.1(b). Effect of fw on microrotation

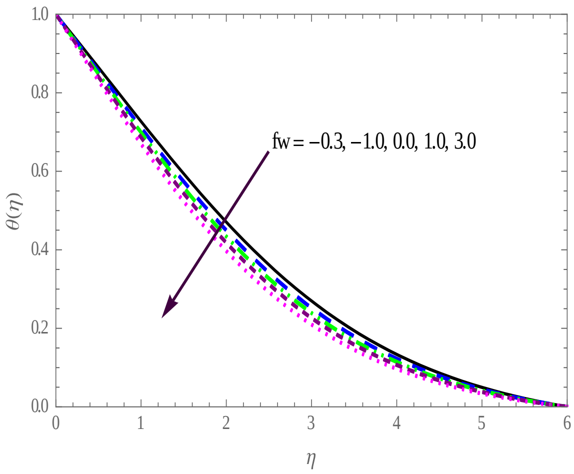

Fig.1(c). Effect of fw on temperature

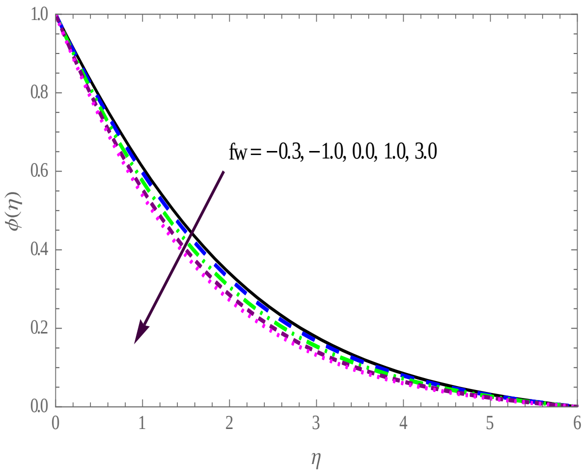

Fig.1(d). Effect of fw on concentration

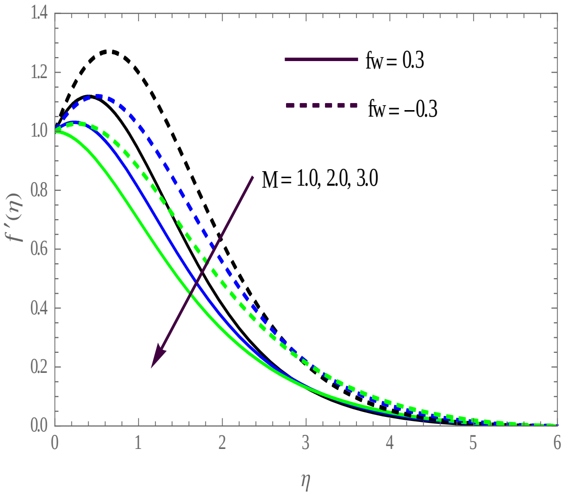

Fig.2(a). Effect of M on velocity

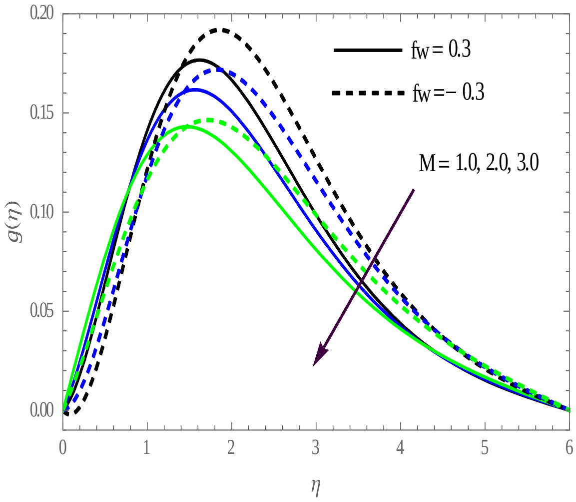

Fig. 2(b). Effect of M on microrotation

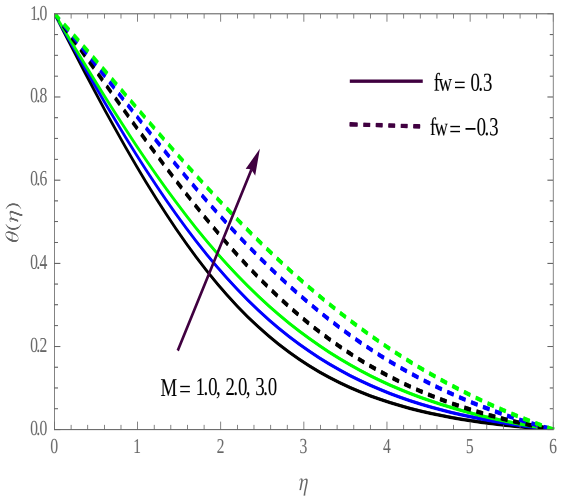

Fig. 2(c). Effect of M on temperature

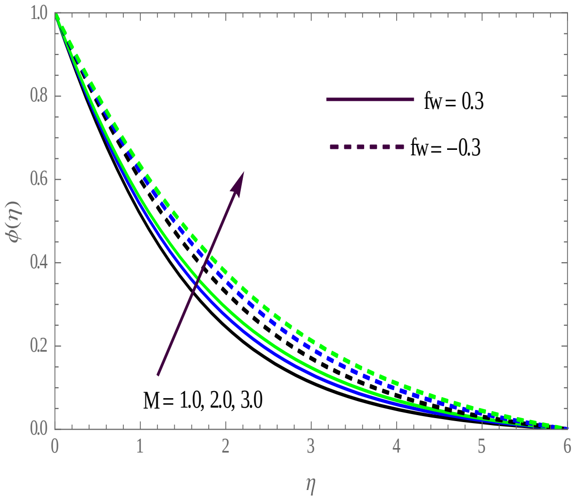

Fig. 2(d). Effect of M on concentration

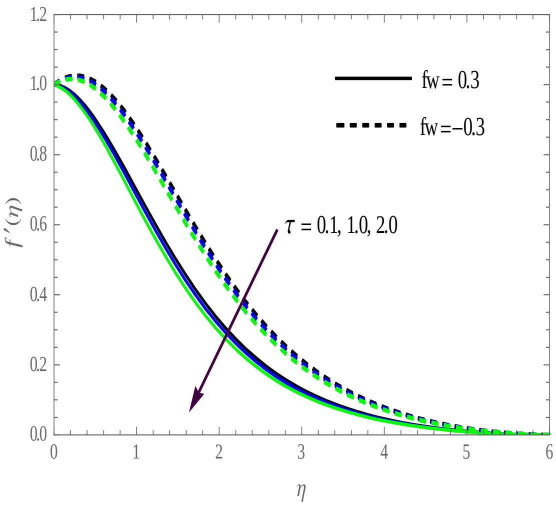

Fig. 3(a) Effect of τ on velocity

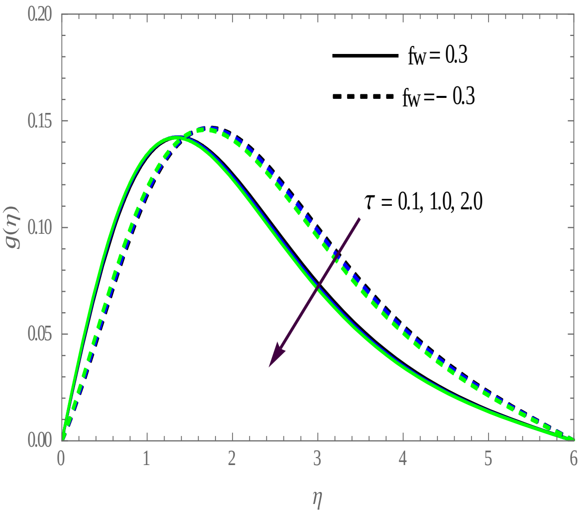

Fig. 3(b). Effect of τ on microrotation

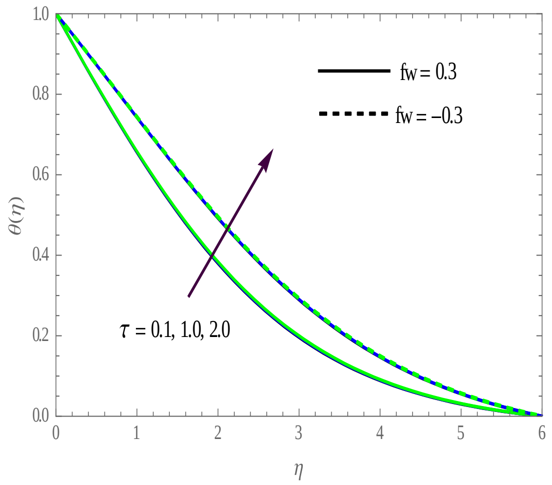

Fig.3(c). Effect of τ on temperature

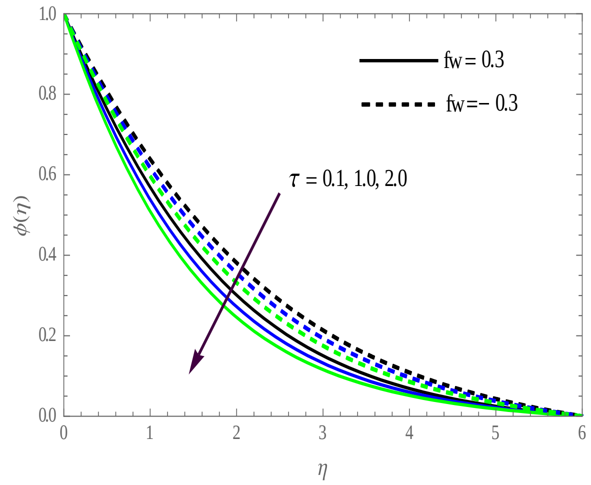

Fig. 3(d). Effect of τ on concentration

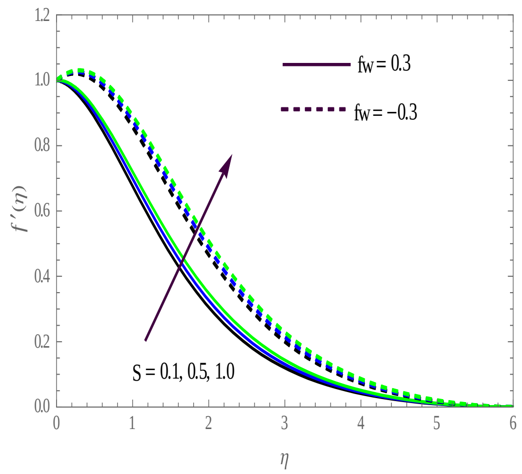

Fig. 4(a) Effect of s on velocity

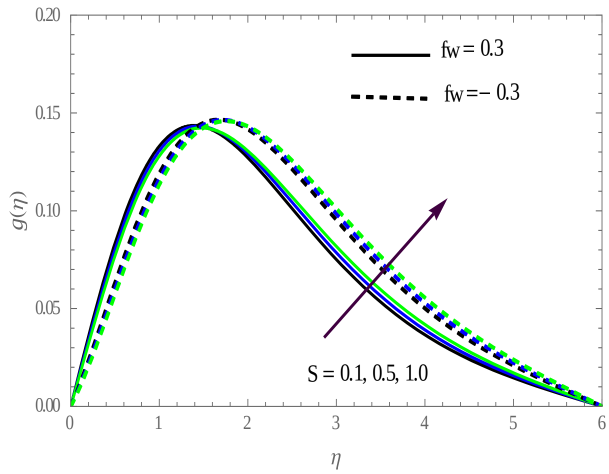

Fig. 4(b). Effect of s on microrotation

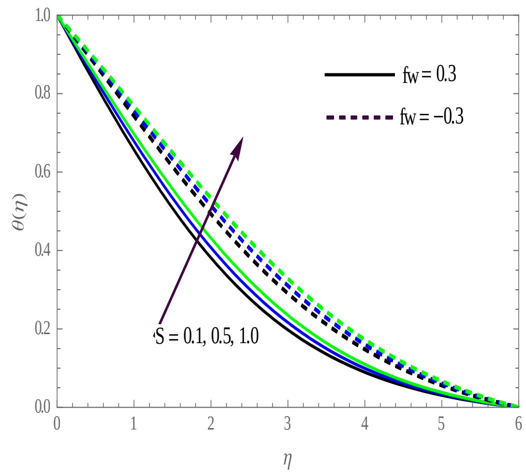

Fig.4(c) Effect of s on temperature

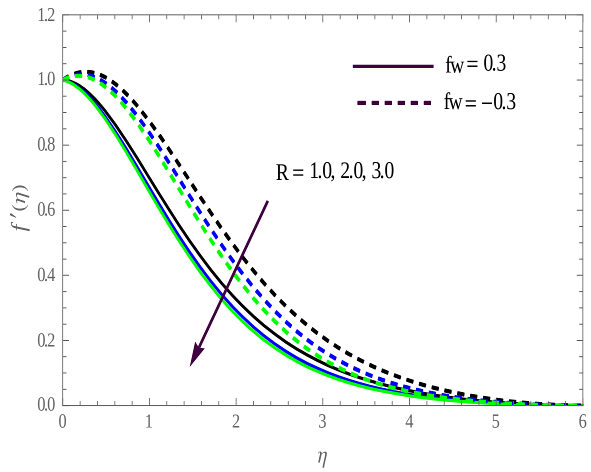

Fig.5(a). Effect of R on velocity

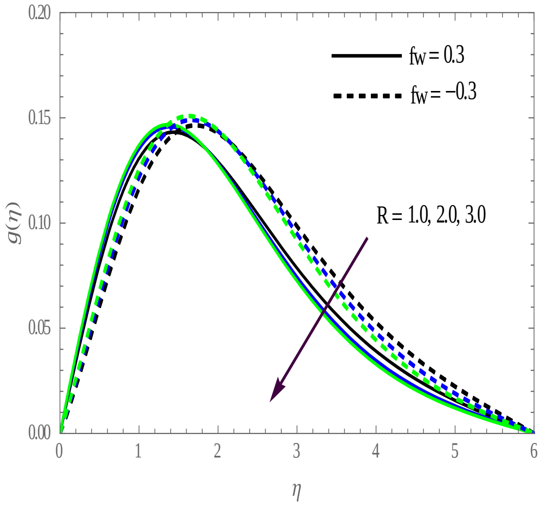

Fig. 5(b). Effect of *R* on microrotation

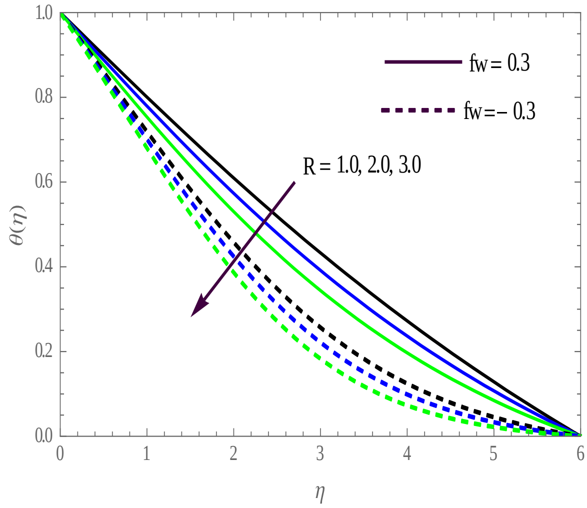

Fig. 5(c) Effect of *R* on temperature

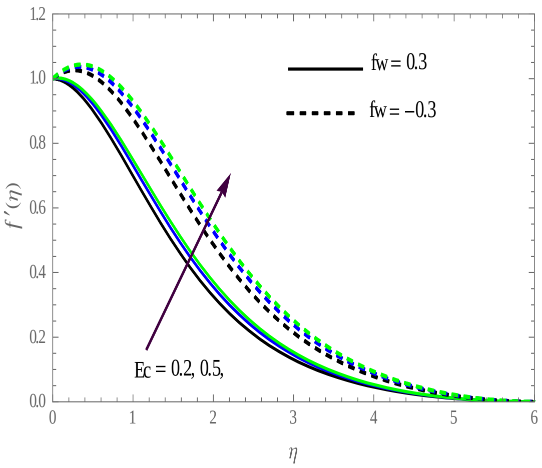

Fig. 6(a) Effect of *Ec* on velocity

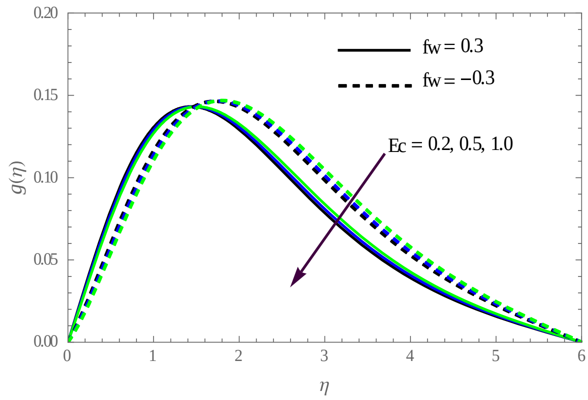

Fig.6(b) Effect of *Ec* on microrotation

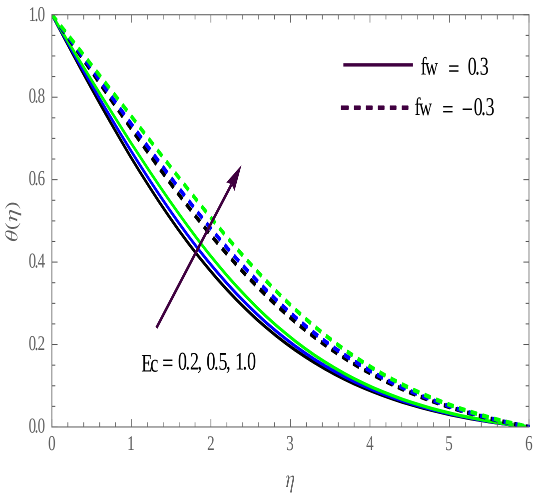

Fig.6(c) Effect of *Ec* on temperature

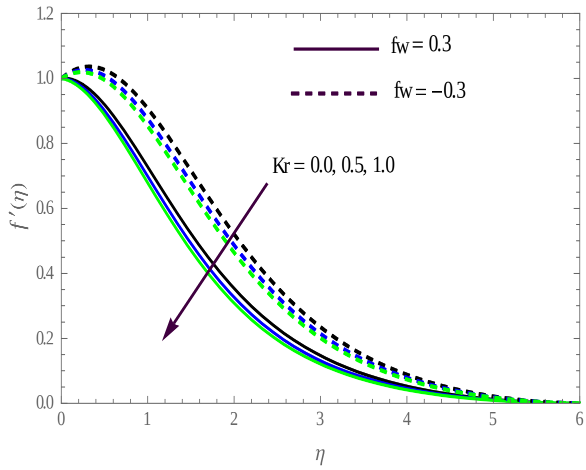

Fig.7(a). Effect of *Kr* on velocity

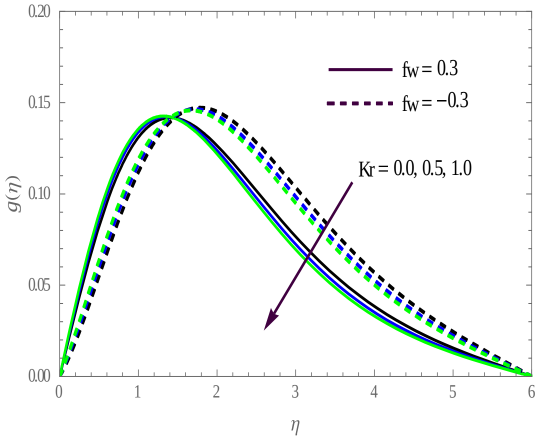

Fig. 7(b). Effect of *Kr* on microrotation

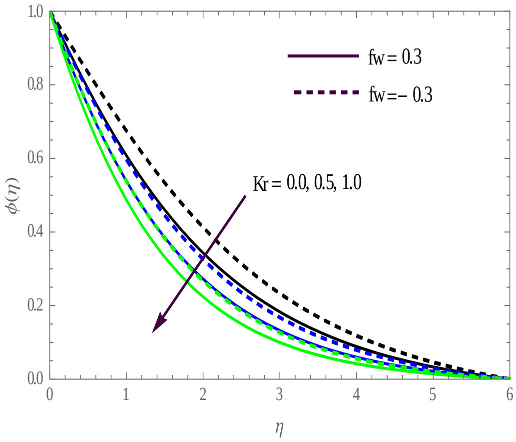

7(c). Effect of *Kr* on concentration

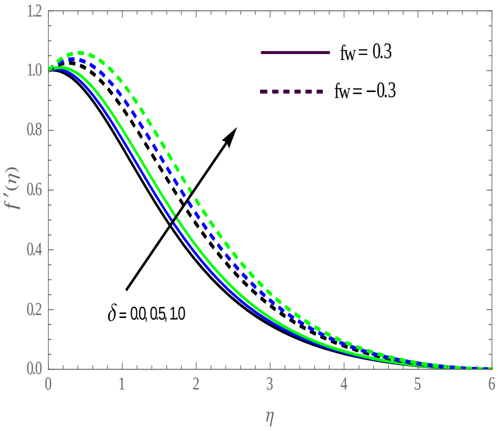

8(a). Effect of δ on velocity

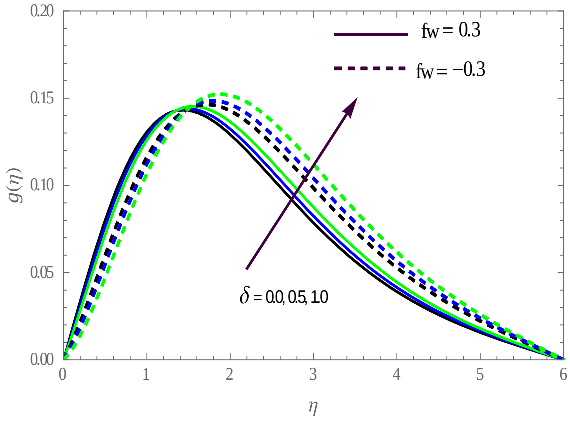

Fig. 8(b). Effect of δ on microrotation

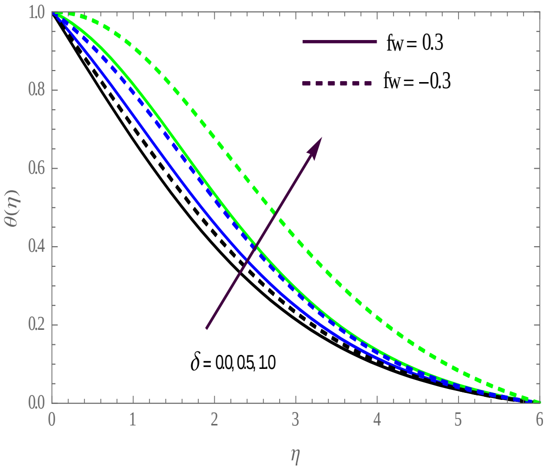

Fig. 8(c). Efect of δ on temperature

Table 1: Various values of $-f''(0)$, $\omega'(0)$, $-\theta'(0)$, $-\phi'(0)$ with $fw = 0.3$ $G_1 = 1.0,\ K = 2.0,\ Gr = 1.0, Gc = 1.0, M = 1.0, \Pr = 0.71, Sc = 0.22.$

M	S	R	τ	Kr	δ	$-f''(0)$	$\omega'(0)$	$-\theta'(0)$	$-\phi'(0)$

1.0	1.0	1.0	1.0	0.5	0.5	1.420038	0.179025	0.304299	0.372532
2.0						1.399627	0.237252	0.264226	0.375292
3.0						1.382628	0.285132	0.240495	0.381126
1.0	1.0	1.0	1.0	0.5	0.5	1.420038	0.179025	0.304299	0.372532
	2.0					1.368912	0.172776	0.345996	0.368695
1.0	3.0					1.342940	0.167093	0.384807	0.365435
1.0	1.0	1.0	1.0	0.5	0.5	1.420038	0.179025	0.304299	0.372532
		2.0				1.365619	0.188929	0.345996	0.368695
		3.0				1.300212	0.195004	0.384807	0.365435
1.0	1.0	1.0	1.0	0.5	0.5	1.420038	0.179025	0.373382	0.370172
			2.0			1.358033	0.181576	0.340074	0.371327
			3.0			1.322152	0.184053	0.304299	0.372532
				0.5	0.5	1.204576	0.179025	0.373382	0.370172
1.0	1.0	1.0	1.0	1.0		1.325645	0.187625	0.340074	0.371327
				1.5		1.442152	0.192341	0.304299	0.372532
				0.5	0.0	1.360028	0.181124	0.285298	0.376532
1.0	1.0	1.0	1.0	0.5	0.5	1.420038	0.179025	0.304299	0.372532
					1.0	1.488912	0.175316	0.326986	0.368095

Table 2: Various values of $-f''(0), \omega'(0), -\theta'(0), -\phi'(0)$ with $fw = -0.3$
$G_1 = 1.0,\ K = 2.0,\ M = 1.0, Gr = 1.0, Gc = 1.0, \Pr = 0.71, Sc = 0.22.$

M	S	R	τ	Kr	δ	$-f''(0)$	$\omega'(0)$	$-\theta'(0)$	$-\phi'(0)$
1.0	1.0	1.0	1.0	0.5	0.5	1.355315	0.105398	0.304299	0.372532
2.0						1.353483	0.173331	0.264226	0.375292
3.0						1.351025	0.228557	0.240495	0.381126
1.0	1.0	1.0	1.0	0.5	0.5	1.355315	0.105398	0.304299	0.372532
	2.0					1.348912	0.100374	0.345996	0.368695
	3.0					1.342940	0.098685	0.384807	0.365435
1.0	1.0	1.0	1.0	0.5	0.5	1.355315	0.105398	0.304299	0.372532
		2.0				1.365619	0.112315	0.345996	0.368695
		3.0				1.372002	0.116605	0.384807	0.365435
1.0	1.0	1.0	1.0	0.5	0.5	1.355315	0.105398	0.373382	0.370172
			2.0			1.367422	0.107523	0.340074	0.371327
			3.0			1.375694	0.109612	0.304299	0.372532
1.0	1.0	1.0	1.0	0.5	0.5	1.355315	0.105398	0.373382	0.370172
				1.0		1.351186	0.113426	0.340074	0.371327
				1.5		1.344268	0.118461	0.304299	0.372532
					0.0	1.420038	0.179025	0.304299	0.372532

1.0	1.0	1.0	1.0	0.5	0.5	1.360038	0.179025	0.304299	0.372532
					1.0	1.301038	0.179025	0.304299	0.372532

In this paper, the effect of suction/injection on a steady magnetohydrodynamic free convective heat and mass transfer flow of incompressible micropolar fluid past a continuous moving plate in the presence of thermal radiation and viscous dissipation has been investigated using Runge-Kutta fourth order technique along with shooting method. In order to get a physical insight of the problem, a parametric study is carried out to illustrate the effect of various thermophysical parameters fw, M, τ, S, R, Ec and Kr on the velocity, microrotation, temperature, concentration, local skin friction, couples stress, local Nusselt number and Sherwood number and are presented in figures and tables.

Figs. 1(a)-(d) depict the velocity, microrotation, temperature and concentration profiles for various values of the suction parameter fw, respectively. It is seen from these figures that as the suction parameter fw increases, there is a fall in the velocity, temperature and concentration as well as their boundary-layer thicknesses, but there is increases in the microrotation near the plate and then decreases away from the plate.

Figs. 2(a)-(d) display the influence of the magnetic field parameter M on the velocity, microrotation, temperature and the concentration, respectively. The presence of a magnetic field has the tendency to produce a drag-like force called the Lorentz force which acts in the opposite direction of the fluid's motion. This causes the fluid velocity and microrotation to decrease and the fluid temperature and concentration to increase as the magnetic field parameter M increases. In addition, the boundary-layer thickness decreases while the thermal boundary-layer thickness increases as M increases. It is also observed from Fig. 2(b) that with an increase in M, the microrotation first increases near the plate and then gradually decreases away from the plate for both the cases of suction as well as injection. From Fig. 2(c) it is seen that M results in a decrease in the temperature. From Fig. 2(d), it is noticed that as the magnetic field parameter M increases, the concentration increases.

The effect of the thermophoretic parameter τ on the velocity, microrotation, temperature and the concentration are depicted in Figs. 3(a)–(d), respectively. It is observed from Fig. 3(a) that the fluid velocity decreases with increase in the thermophoretic parameter and so the momentum boundary layer thickness decreases. It is also observed that duo to an increase in thermophoretic parameter τ, the microrotation first increases near the surface and then gradually decreases for both the cases of suction as well as injection in sketched in Fig. 3(b). From Fig. 3(c) it is also seen that τ results in a decrease in the temperature. In the boundary layer region, the concentration of the fluid decreases with increasing the values of thermophoretic parameter as depicted in Fig.3(d). So, thermophoretic parameter τ is expected to alter the concentration boundary layer.

Figs. 4(a)–(c) illustrate the velocity, microrotation and temperature profiles, for variation in the thermal conductivity parameter S for both suction as well as injection. Fig. 4(a) shows that an increase in thermal conductivity parameter tends to increase the fluid velocity in the boundary layer region. The physics behind the results is that the thermal conductivity parameter increases the thickness of momentum boundary layer, which ultimately enhances the velocity. Fig. 4(b) it is observed that as R increases, the microrotation increases near the plate and decreases away from the plate. From Fig. 4(c), it is also seen that the temperature increases with increasing S. Thus, by rising in thermal conductivity parameter S, thermal boundary layer thickness enhances.

Figs. 5(a)–(c) illustrate the velocity, microrotation and temperature profiles, for variation in the thermal radiation parameter R for both suction as well as injection. Fig. 5(a) shows that an increase in radiation parameter tends to increase the fluid velocity in the boundary layer region. The physics behind the results is that the thermal radiation increases the thickness of momentum boundary layer, which ultimately enhances the velocity. Fig. 5(b) it is clearly seen that as *R* increases, the microrotation increases near the plate and decreases away from the plate. From Fig. 5(c), it is also observed that the temperature distribution increases uniformly with increasing thermal radiation parameter *R*. Thus, by escalating *R*, thermal boundary layer thickness enhances.

The effect of viscous dissipation parameter i.e., Eckert number *Ec* on the velocity, microrotation and temperature are illustrated in Figs. 6(a)-(c), respectively. Fig. 6(a) shows that the velocity field increases with the increase of *Ec* for fluid suction as well as for injection. Fig. 6(b) displays that the microrotation increases near the plate and then decreases away from the plate with the increase of *Ec* for fluid suction as well as for injection. Fig. 6(c) also, shows that the temperature increases with increasing values of *Ec* for fluid suction as well as for injection.

Figs. 7(a)-(c), illustrate the dimensionless velocity, microrotation and concentration profiles for various values of the chemical reaction parameter *Kr*. From Fig. 7(a), it is noted that the velocity decreases as *Kr* increases for both the cases of constant fluid suction or injection. Fig. 7(b) shows that as *Kr* increases, first the microrotation increases near the plate and then decreases away from the plate for both the cases of constant fluid suction and injection. Further, from Fig. 7(c) it is also seen that concentration increases as *Kr* increases for both the cases of constant fluid suction and injection.

Figs. 8(a)-(c), illustrate the dimensionless velocity, microrotation and temperature profiles for various values of the heat generation/absorption parameter δ. From Fig. 8(a), it is noted that the velocity increases as δ increases for both the cases of constant fluid suction or injection. Fig. 8(b) shows that as δ increases, first the microrotation decreases near the plate and then increases away from the plate for the cases of constant fluid suction as well as injection. Further, from Fig. 8(c) it is also seen that the temperature increases as in δ increases for the cases of constant fluid suction or injection.

The effects of all pertinent physical parameters on the local skin friction coefficient, couple stress coefficient, the local Nusselt number and the local Sherwood number for the both the cases of constant fluid suction and injection are shown in Table 1 and 2, respectively. From this table, we can see that the skin friction coefficient rises as *Kr*, whereas it reduces with the increment in *S*, *R,* δ and τ for fluid suction as well as for injection. Couple stress coefficient increases as *M*, *R*, τ and *Kr*, whereas it decreases with the increment values in *S* and δ for fluid suction as well as for injection. Nusselt number increases as *M*, *R* whereas it decreases with the increment values in *M*, τ and *Kr* for both fluid suction and injection, But they have opposite behavior on the Sherwood number for fluid suction as well as for injection.

4. CONCLUSIONS

The present work helps us understanding numerically as well as physically the thermophoresis phenomenon on heat and mass transfer flow of Newtonian fluid past an inclined permeable surface in the presence of magnetic field and thermal radiation with viscous and magnetic dissipations. Based on the obtained graphical results, the following conclusions may be drawn:

1. Increasing magnetic field strength decreases the wall shear stress, rate of heat transfer and mass deposition flux from the radiate porous surface. Magnetic field significantly controls the flow, heat, and mass transfer characteristics.
2. Increasing radiation parameter leads to decrease the hydrodynamic as well as thermal boundary layer thickness whereas increases the concentration boundary layer thickness.
3. The heat transfer rate is decreased due to viscous dissipation as it works like a heat source.
4. Increasing thermophoretic parameter decreases the concentration as well as the local Stanton number inside the boundary layer.

In this work, the results indicate that the magnetic parameter has the effect of increasing the value of the skin-friction and reducing the rate of heat transfer. However, the radiation parameter and the surface temperature parameter, have the effect of increasing the value of the Nusselt number, while the thermal conductivity parameter has the opposite effect on the Nusselt number.

5. REFERENCES

[1]. Z. Tadmor, I. Kelin, Engineering principles of plasticating extrusion, in: Polymer Science and Engineering Series, Van Nostrand Reinhold, New York, 1970.
[2]. E.G. Fisher, Extrusion of Plastic, Wiley, New York, 1976.
[3]. T. Altan, S. Oh, H. Gegel, Metal Forming Fundamentals and Applications, American Society of Metals Park, OH, 1979.
[4]. B.C. Sakiadis, Boundary-layer behavior on continuous solid surfaces, AIChE J. 7 (1961) 26–28.
[5]. L.E. Erickson, L.T. Fan, V.G. Fox, Heat and mass transfer on a moving continuous flat plate with suction or injection, Ind. Eng. Chem. Fund. 5 (1969), 19–25.
[6]. V.G. Fox, L.E. Erickson, L.T. Fan, The laminar boundary layer on a moving continuous flat sheet immersed in a non-Newtonian fluid, Am. Inst. Chem. Eng. J. 15 (1969), 327–333.
[7]. L.J. Crane, Flow past a stretching plate, ZAMP 21 (1970), 645–647.
[8]. P.S. Gupta, A.S. Gupta, Heat and mass transfer on a stretching sheet with suction or blowing, Can. J. Chem. Eng. 55 (1977), 744–746.
[9]. C.K. Chen, M.I. Char, Heat transfer on a continuous stretching surface with suction or blowing, J. Math. Anal. Appl. 135 (1988), 568–580.
[10]. A. Chakrabarti, A.S. Gupta, Hydromagnetic flow heat and mass transfer over a stretching sheet, Q. Appl. Math. 37 (1979), 73–78.
[11]. A.C. Eringen, Theory of micropolar fluids, Math. Mech. 6 (1966), 1–18.
[12]. A.C. Eringen, Theory of thermomicro fluids, Math. Anal. 38 (1972), 480–496.
[13]. G. Ahmadi, Self-similar solution of incompressible micropolar boundary layer flow over a semi-infinite plate, Int. J. Eng. Sci. 14, (1976), 639–646.
[14]. R.S.R. Gorla, R. Pender, J. Eppich, Heat transfer in micropolar boundary layer flow over a flat plate, Int. J. Eng. Sci. 19 (1983), 1431–1439.
[15]. V.M. Soundalgekar, H.S. Takhar, Flow of micropolar fluid past a continuously moving plate, Int. J. Eng. Sci. 21 (1983), 961–965.
[16]. H.S. Takhar, V.M. Soundalgekar, Flow and heat transfer of micropolar fluid past a porous plate, Indian. J. Pure Appl. Math. 16 (5), (1985), 552–558.
[17]. R.S.R. Gorla, Combined forced and free convection in the boundary layer flow of a micropolar fluid on a continuous moving vertical cylinder, Int. J. Eng. Sci. 27 (1) (1989), 77–86.
[18]. I.A. Hassanien, R.S.R. Gorla, Heat transfer to a micropolar fluid from a non-isothermal stretching sheet with suction and blowing, Acta Mech. 84 (1990), 191–199.
[19]. H.S. Takhar, R.S. Agarwal, R. Bhargava, S. Jain, Mixed convection flow of a micropolar fluid over a stretching sheet, Heat Mass Transfer 34 (1998), 213–219.
[20]. M.A. Mansour, R.S.R. Gorla, Micropolar fluid flow past a continuously moving plate in the presence of magnetic field, Appl. Mech. Eng. 4 (1999), 663–672.
[21]. M.A. Mansour, A.A. Mohammadein, S.M.M. El-Kabeir, R.S.R. Gorla, Heat transfer from moving surface in a micropolar fluid, Can. J. Phys. 77 (1999), 463–471.
[22]. F.S. Ibrahim, F.M. Hady, Mixed convection-radiation interaction in boundary-layer flow over horizontal surface, Astrophys. Space Sci. 168 (1990), 263–276.
[23]. A. Raptis, Flow of a micropolar fluid past a continuously moving plate by the presence of radiation, Int. J. Heat Mass Transfer 41 (1998), 2865–2866.
[24]. A. Raptis, Radiation and viscoelastic flow, Int. Commun. Heat Mass Transfer 26 (1999), 880–895.
[25]. H.A.M. El-Arabawy, Effect of suction/injection of the flow of a micropolar fluid past a continuously moving plate in the presence of radiation, Int. J. Heat Mass Transfer 46 (2003), 1471–1477.
[26]. A. Raptis, C. Perdikis, H.S. Takhar, Effect of thermal radiation on MHD flow, Appl. Math. Comput. 153 (2004), 645–649.
[27]. P.G. Siddheshwar, U.S. Mahabaleswar, Effect of radiation and heat source on MHD flow of a viscoelastic liquid and heat transfer over a stretching sheet, Int. J. Non-Linear Mech. 40 (2005), 807–820.
[28]. Duwairi H. M., Damesh R. A., (2008), Effects of thermophoresis particle

deposition on mixed convection from vertical surfaces embedded in saturated porous medium, Int. J. Numer. Meth. Heat Fluid Flow, 18(2), pp. 202-216.

[29]. Rahman M.M., Alam M.S. and Chowdhury M.K., (2012), Local similarity solutions for unsteady two dimensional forced convective heat and mass transfer flow along a wedge with thermophoresis, Int. J. Appl. Math and Mech, 8 (8), pp. 96-112.

[30]. Postelnicu A., Thermophersis partical deposition in natural convection over inclined surfaces in porus media, Int. J. Heat and Mass Transfer, (2012) 55, pp. 2087-2094.

[31]. Das U.N. Deka R.K and Soundalgekar V.M. (1994). Effects of Mass Transfer on Flow past an Impulsively Started Infinite Vertical Plate with Constant Heat Flux and Chemical reaction, *Forschung im Ingenieurwesen*, 60(10): 284-287.

[32]. Muthucumarswamy R and Ganesan P(2001). First Order Chemical Reaction on Flow past an Impulsively Started Vertical Plate with Uniform Heat and Mass Flux, *Acta Mechanica*, 147(1): 45-57.

[33]. Muthucumarswamy R, (2002). Effects of a Chemical Reaction on Moving Isothermal Vertical Surface with Suction, *Acta Mechanica*, 155(1-2): 65-70.

[34]. Ibrahim F.S. Elaiw A.M. and Bakr A.A (2008). Effect of the chemical reaction and radiation absorption on the unsteady MHD free convection flow past a semi-infinite vertical permeable moving plate with heat source and suction, *communications in Non-linear Science and Numerical Simulation* 13: 1056-1066.

[35]. Damseh R.A., Al-Odata M.Q., Chamkha A.J.and Shannak B.A. (2009). Combined effect of heat generation or absorption and first-order chemical reaction on micropolar fluid flows over a uniformly stretched permeable surface. *Int. J. Thermal Sci.* 48: 1658-1663.

[36]. Pal D and Talukdar B, (2010a). Perturbation analysis of unsteady magnetohydrodynamic convective heat and mass transfer in a boundary layer slip flow past a vertical permeable plate with thermal radiation and chemical reaction, *Commu. Non- linear Sci. Numer. Simulation.,* 15: 1813–1830.

[37]. Pal D and Talukdar B, (2010b). Buoyancy and chemical reaction effects on MHD mixed convection heat and mass transfer in a porous medium with thermal radiation and Ohmic heating. Commun. Nonlinear Sci. Numer. Simul. 15: 2878–2893.

[38]. Ghaly A.Y, Seddeek M.A. (2004). Chebyshev finite difference method for the effect of chemical reaction, heat and mass transfer on laminar flow along a semiinfinite horizontal plate with temperature dependent viscosity. *Choas Solitons Fractals* 19: 61–70.

[39]. J.C. Slattery, Momentum, Energy and Mass Transfer in Continua, McGraw-Hill, New York, 1972.

[40]. Postelnicu A., Thermophersis partical deposition in natural convection over inclined surfaces in porus media, Int. J. Heat and Mass Transfer, (2012) 55, pp. 2087-2094.

[41]. Talbot L, Cheng R.K, Schefer A.W, Wills D.R. Thermophoresis of particles in a heated boundary layer. J Fluid Mech 1980; 101:737-758.

[42]. Batchelor G.K, Shen C. Thermophoretic deposition of particles in gas flowing over cold surface. J Colloid Interface Sci 1985; 107:21-37.

[43]. Mills A.F, Hang X, Ayazi F., The effect of wall suction and thermophoresis on aerosol-particle deposition from a laminar boundary layer on a flat plate, Int. J. Heat Mass Transfer 27 (1984) 1110–1114.

[44]. J.C. Slattery, Momentum, Energy and Mass Transfer in Continua, McGraw-Hill, New York, 1972.

[45]. E.M. Sparrow, R.D. Cess, Radiation Heat Transfer, Hemisphere Publishing Corporation, Washington, DC, 1978.

[46]. H. Schlichting, Boundary Layer Theory, McGraw-Hill, New York, 1968.